ACS Sustainable Chemistry & Engineering

Research Article

pubs.acs.org/journal/ascecg

Fruit Peels as Efficient Renewable Adsorbents for Removal of Dissolved Heavy Metals and Dyes from Water

Ramakrishna Mallampati,[†] Li Xuanjun,[‡] Avner Adin,[†] and Suresh Valiyaveettil*[,‡]

[†]NUS Environmental Research Institute, National University of Singapore, T-Lab Building, 5A Engineering Drive 1, Singapore 117411, Singapore

[‡]Department of Chemistry, National University of Singapore, 3 Science Drive 3, Singapore 117543, Singapore

Supporting Information

ABSTRACT: Removal of heavy metal ions and dissolved organic compounds present in wastewater is a challenge for many countries owing to high cost of existing technologies and continued increase in water consumption. In this study, three natural materials, avocado, hamimelon and dragon fruit peels, were selected and used as simple and renewable adsorbents for water purification. The presence of surface functional groups such as $-CO_2H$, $-OH$ and morphologies of the peels were characterized using spectroscopic and electron microscopic techniques, respectively. All peals were effective toward removing dyes and toxic metal ions from water. The extraction capacity of peels increased with extraction time and a plateau was reached at equilibrium. Dragon fruit peels showed highest extraction efficiency toward alcian blue (71.85 mg/g) and methylene blue (62.58 mg/g). Hamimelon peels and avaocado peels showed moderate extraction capacity for Pb^{2+} (7.89 mg/g, 9.82 mg/g) and Ni^{2+} (9.45 mg/g, 4.93 mg/g) cations. The Langmuir isotherm model was useful to explain the adsorption process, dominated by electrostatic interaction between adsorbent and adsorbates, indicating a monolayer adsorption at the binding sites on the surface of the peels. However, the adsorption model for methylene blue and neutral red is still a matter of conjecture. The adsorbents can be regenerated at acidic pH and could reuse for a few cycles.

KEYWORDS: *Biopeels, Water purification, Pollutants, Bioadsorbents, Adsorption, Extraction*

INTRODUCTION

One of the major problems faced by many countries around the world is the dwindling supply of safe and clean drinking water.[1] The increase in industrial activities releases effluents containing pollutants such as heavy metal ions, organic dyes and pharmaceuticals into the aquatic environment, which cause significant health hazards to living organisms and overall deterioration of the environment.[2−8] Because most of the organic molecular pollutants are stable, small in size and not biodegradable, it is difficult to eliminate them from wastewater.[9] Many water purification methods such as chemical coagulation, photodegradation, precipitation, flocculation, activated sludge, membrane separation and ion exchange processes have been tested for removing the pollutants.[2,4,10,11] Yet, it is difficult to find a single effective method that can remove all harmful pollutants from water. Compared to conventional water purification methods, use of bioadsorbents could be advantageous owing to the low cost, ready availability, environmental friendliness and high efficiency.[5] Various bioadsorbents such as banana peels,[12] orange peels,[2,12,13] rice husk,[10] tea waste,[14,15] sugarcane bagasse,[16] pine bark[17] and other peels[18−25] were tested for the extraction of heavy metal ions and dyes from water. A notable disadvantage of such biopeels is the release of soluble organic compounds into water, which limits their use in large scale applications. Efficient and universal low cost adsorbents that will not produce a secondary water contamination during the purification process are to be developed.

Owing to the multifunctional characteristics of biopeels, adsorption of pollutants is facilitated by a combination of processes, involving ion exchange, complexation and electrostatic interactions.[13] Locally available avocado (AV), hamimelon (HM) and dragon (DF) fruits were selected for the this study based on cost, easy availability, processing methods, stability and potential ability to extract different pollutants. All fruit peels contain polar functional groups such as $-OH$, $-NH_2$ and $-COOH$ on the surface.[24,26] To test the effectiveness, extractions of heavy metal ions (Pb^{2+}, Ni^{2+} and $Cr_2O_7^{2-}$) and dyes (alcian blue, methylene blue, neutral red and brilliant blue) from aqueous solutions were carried out using the peels and analyzed the data (Scheme 1).

MATERIALS AND METHODS

Alcian blue (AB), coomassie brilliant blue G-250 (BB), neutral red (NR) and methylene blue (MB), potassium dichromate ($K_2Cr_2O_7$), lead nitrate ($Pb(NO_3)_2$) and nickel nitrate ($Ni(NO_3)_2{\cdot}6H_2O$), hydrochloric acid (HCl) and sodium hydroxide (NaOH) were

Received: January 19, 2015
Published: April 8, 2015

DOI: 10.1021/acssuschemeng.5b00207
ACS Sustainable Chem. Eng. 2015, 3, 1117−1124

Scheme 1. Schematic Representation of the Extraction of Dyes from Aqueous Solutions Using Fruit Peels

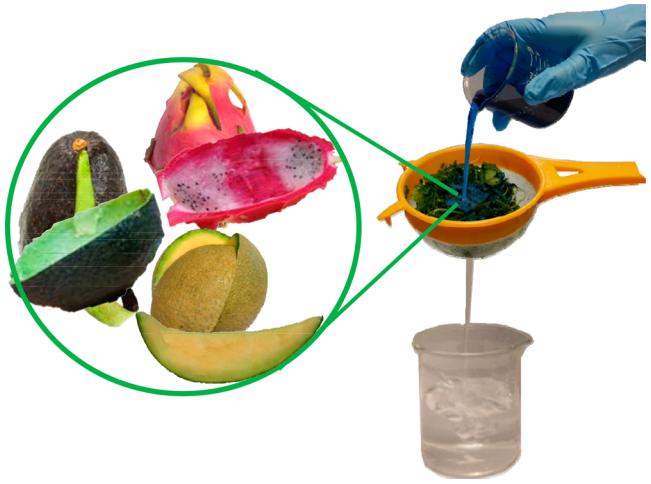

purchased from Sigma-Aldrich and used without further purification. Ultrapure water was used for all syntheses and preparation of stock solutions by dissolving appropriate amounts of corresponding chemicals in water.

Preparation of Biopeel Adsorbent. Hamimelon, avocado and dragon fruits were bought from a local supermarket, washed thoroughly with water, peeled the outer layer and cut into small pieces of around 0.04 cm^2 in size. Raw peels were saponified with NaOH to cleave ester bonds on the surface of peels to generate more hydoxyl groups, followed by thorough washing with deionized water to remove excess base. Washed peels were sonicated in 2-proponol to extract soluble organics and then filtered, washed with water and dried.

Characterization Methods. Surface morphology of the treated peels was established using field emission scanning electron microscopy (FESEM, JEOL JSM-6701F). Energy dispersive X-ray spectroscopy (EDS) was used to investigate the chemical composition of fruit peel surface. The IR spectra were recorded in the range of 4000−400 cm^{-1} using a Bruker ALPHA FT-IR (Fourier transform infrared) spectrophotometer using KBr as a matrix. The concentrations of metal pollutants in experimental and control samples were analyzed using inductively coupled plasma optical emission spectroscopy (ICP-OES, Dual-view Optima 5300 DV ICP-OES system). Quantification of dye solutions was carried out using a UV−vis spectrophotometer (Shimadzu-1601 PC spectrophotometer). Carbon, hydrogen, nitrogen and sulfur (CHNS) analyses were done using an Elementar Vario Micro Cube instrument.

Batch Adsorption Studies. *Effect of Initial Adsorbate Concentration and Time.* Adsorbent (0.1 g) was added to solutions (10 mL) of pollutants at different concentrations. All adsorption experiments were done at 30 °C using an orbital shaker operating at 200 rpm. The residual concentrations of pollutants were analyzed after predetermined intervals of time until the system reached equilibrium. The pollutant adsorbed at equilibrium q_e (mg/g) was calculated using the following equation:

$$q_e = (C_0 - C_e)V/M \quad (1)$$

where C_0 and C_e (mg/L) are concentrations of pollutant at initial stage and equilibrium conditions, V (L) is volume of the pollutant solution and M (g) is mass of the adsorbent used. The initial concentrations of pollutant solution tested were 5, 10, 20, 40, 70, 100 and 200 mg/L, and the experiments were carried out at 30 °C for 24 h.

Effect of Solution pH. The effect of pH on pollutant extraction was studied by varying the pH from 2 to 12, where the pH was adjusted by adding either 0.01 N HCl or 0.01 N NaOH solution. The initial concentrations of cationic pollutants (AB, Pb^{2+} and Ni^{2+}) used for this study were 100 and 20 mg/L for anionic pollutants (chromate anion, BB, NR and MB). Other parameters such as adsorbent dosage, agitation speed and solution temperature remained constant. The percentage removal of pollutant was calculated as

$$\text{removal}\% = \left(\frac{C_i - C_f}{C_i}\right)100 \quad (2)$$

where C_i and C_f (mg/L) are initial and final pollutant concentrations in water, respectively.

RESULTS AND DISCUSSION

Characterization of Biosorbents. The functional groups on the peels were studied using FT-IR spectrophotometry in the range of 4000 to 400 cm^{-1} (Figure 1).

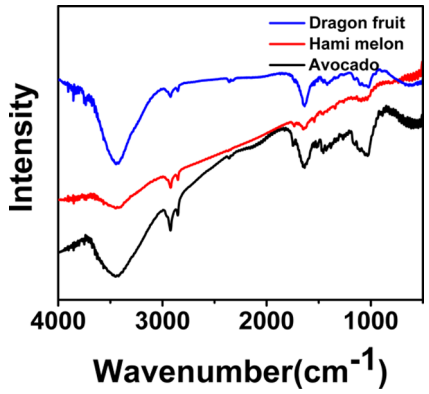

Figure 1. FT-IR spectra of avocado, hamimelon and dragon fruit peels.

The broad band observed at 3200−3650 cm^{-1} for all three peels matches the O—H stretching frequency. The sharp peaks observed at 2928, 2921 and 2926 cm^{-1} in the spectra for biopeels correspond to the C—H stretching frequency.[27] The strong absorption at 1747 cm^{-1} for avocado peel and 1754 cm^{-1} for hamimelon peel are due to the C═O stretching frequency of esters or carboxylic acid functional groups. The peaks in the range of 1680−1610 cm^{-1} correspond to the stretching of the C═C bonds in the aromatic rings present in all three peels. The absorption peaks observed in the range of 1300−1000 cm^{-1} could be accounted to angular deformation in the plane of the C—H bonds of aromatic rings and in the range of 1200−1000 cm^{-1} corresponds to the axial C—O bond in phenols. To elucidate the functional groups involved in the adsorption of pollutants, the FT-IR spectra of a few peels were recorded after adsorption. As expected, no significant differences in the spectra were observed before and after adsorption of pollutants (see Figure S1 of the Supporting Information). The adsorption of pollutants is not expected to cause any functional group transformation on the surface. In the SEM micrographs, surface of washed peels showed an irregular morphology (Figure 2) that is expected with plant based cellulosic materials.[28]

Further, the compositions of all peels were evaluated using elemental analysis (Table 1) showing low nitrogen content. It is conceivable that presence of hydroxyl and carboxyl groups on the surface of biopeels is responsible for the extraction of pollutants from water.

Changes of Pollutant Concentration with Contact Time. *Extraction of Dyes.* All biopeels were evaluated for their binding ability of different pollutants. Graphs of the changes in extraction efficiency (q_t) with time for different pollutants using three peels at room temperature are shown in Figure 3. The adsorption capacity of the pollutants increased with increasing

DOI: 10.1021/acssuschemeng.5b00207
ACS Sustainable Chem. Eng. 2015, 3, 1117−1124

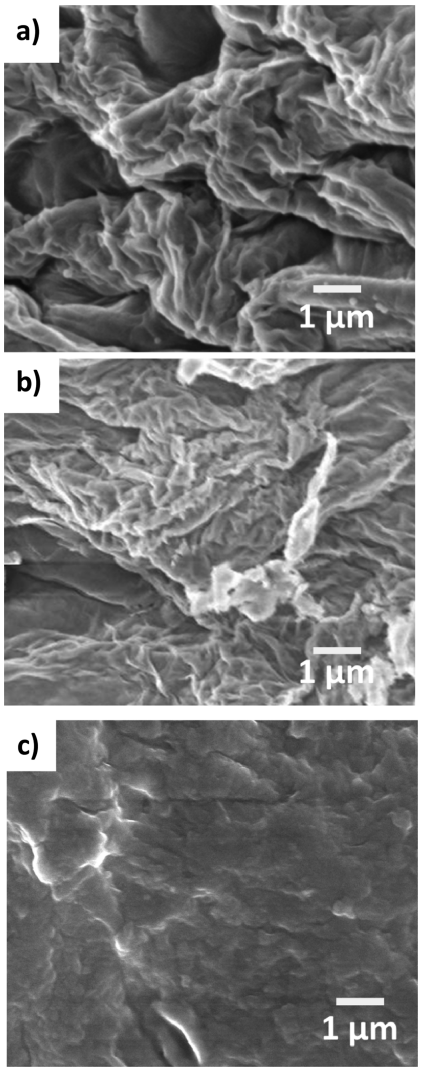

Figure 2. FESEM images of the surface treated avocado (a), hamimelon (b) and dragon fruit (c) peels.

Table 1. Elemental Analysis Data of Different Biosorbents

biopeel	carbon (wt %)	hydrogen (wt %)	nitrogen (wt %)	sulfur (wt %)
avocado	46.38	5.67	0.94	<0.50
hamimelon	39.35	5.14	<0.50	<0.50
dragon fruit	33.14	4.66	1.29	0.58

extraction time and a plateau was reached at equilibrium (60 min). This implies that the adsorption process is rapid in the beginning, gradually decreases as time progresses and finally attains saturation when equilibrium is reached. High adsorption values were obtained for the adsorption of cationic dyes (AB and MB), and all three peels bind cationic dyes more favorably than anionic (BB) and neutral dyes (NR). This might be due to the presence of phenoxide groups and carboxylate groups ($-COO^-$) on the peel surface, which then facilitate the extraction of cationic dyes.[28]

Extraction of Metal Ions. Similar results were observed for metal cations (Pb^{2+} and Ni^{2+}) with higher extraction efficiencies, as compared to the anions (Figure 3d,e,f). It is worth mentioning that all three peels showed good adsorption for Ni^{2+} ions. The avocado peels showed high affinity and

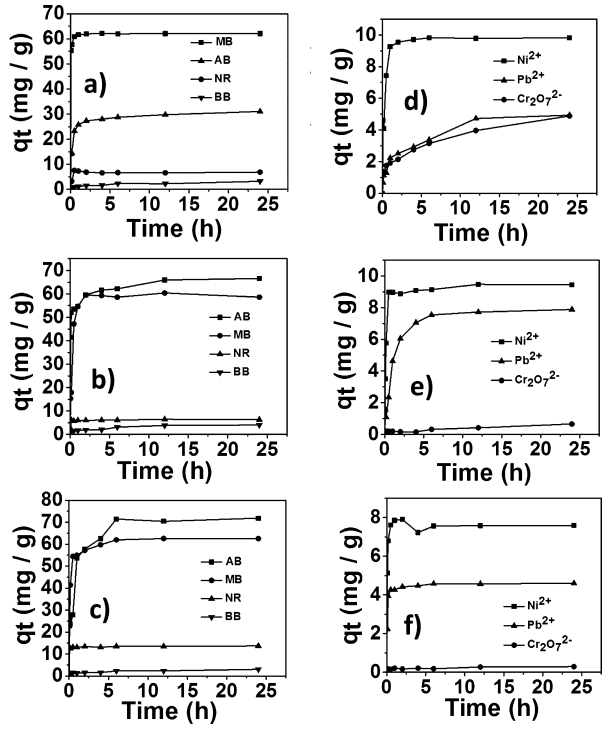

Figure 3. Variation of adsorption capacity of dyes (a, b, c) and heavy metal ions (d, e, f) for avocado (a, d), hamimelon (b, e) and dragon fruit (c, f) peels (pH 7, temperature 25 °C).

extraction efficiency for chromate anions, which might be due to the esterification reaction between the functional groups on the surface of avocado peel and $HCrO_4^-$ ions.[29] Dragon fruit peels were efficient for the extraction of cationic pollutants. Presence of carboxylate groups on the surface facilitated the binding of cationic pollutants rather than the anionic ones. This observation led to the conclusion that adsorption of pollutants involved electrostatic interaction between adsorbent and adsorbates.

Effect of pH on the Adsorption of Different Pollutants. Extraction of Dyes. The extraction data for pollutants using different peels at various solution pH values are shown in Figure 4. The percentage removal of pollutants increased with increasing pH, owing to the efficient exchange of cations with H^+ of $-COOH$ and $-OH$ functional groups. At low pH values (acidic medium), the H^+ ions protonate surface functional groups and compete with the adsorption of other cationic pollutants.[30] However, as the pH values increased, extraction of cations by the negatively charged adsorption sites increased significantly.[31] In addition, at lower pH values with high concentrations of H^+, the positively charged adsorbent surface extracted negatively charged pollutants.

Extraction of Metal Ions. Similarly, extraction of cationic pollutants (Pb^{2+}, Ni^{2+}) over anionic groups ($Cr_2O_7^{2-}$) at higher pH values (Figure 4d,e,f) is explained using the electrostatic interaction between oppositely charged absorbents and adsorbate. The speciation changes of Pb^{2+} and Ni^{2+} ions over a range of pH values were reported in earlier adsorption studies.[32,33] Our data also draw similar conclusions. Adsorption of cations on the peel surface increased with increase in pH. Excess H^+ ions in solution compete with the adsorption of Pb^{2+}, Ni^{2+} ions at low pH values. It should be noted that chromate anions are present in two forms, $HCrO_4^-$ and CrO_4^{2-} ions in aqueous solution. The $HCrO_4^-$ ions are stable and

DOI: 10.1021/acssuschemeng.5b00207
ACS Sustainable Chem. Eng. 2015, 3, 1117−1124

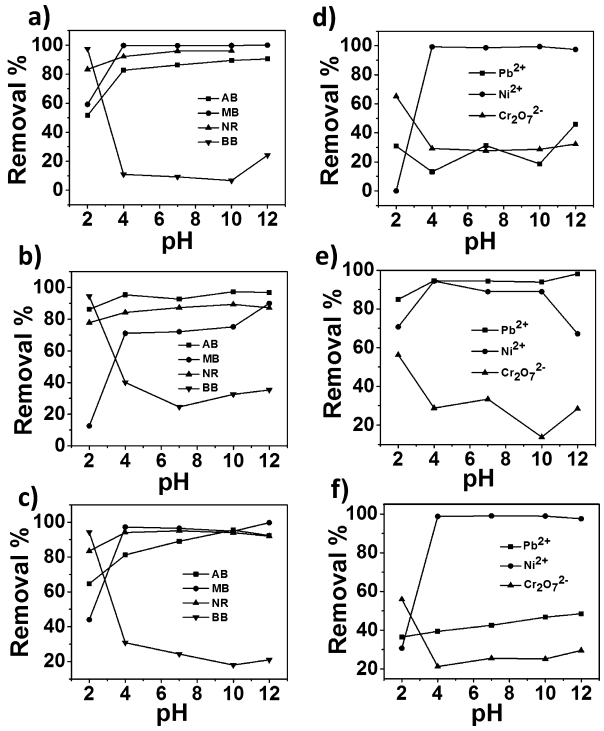

Figure 4. Effect of pH on adsorption capacity of dyes (a, b, c) and heavy metal ions (d, e, f) for avocado (a, d), hamimelon (b, e) and dragon fruit (c, f) peels (temperature 25 °C).

dominant at pH values lower than 5,[34] and chromate anion adsorption decrease as pH increases. Multiple functional groups such as −COOH, −OH on the adsorbent surface facilitate the adsorption of cations at higher pH. Exchange of H^+ with cations is low at acidic pH due to high concentration of H^+. The maximum adsorption capacities of all pollutants using three biopeels are shown in Table 2.

Kinetic Studies. There are several kinetic models proposed for the mechanism by which pollutants are adsorbed on the surface of adsorbents.[18,19] To analyze the adsorption kinetics of the pollutants onto the three peels, the pseudo-first-order and pseudo-second-order kinetic models were used to process the data. Kinetic data plots of avocado peels with different dyes and metal ions are shown in Figure 5, and all data collected for dragon fruit peels and hamimelon peels are given in the Supporting Information (Figures S2−S5)

Pseudo-First-Order Kinetic Model. The linear form of the pseudo-first-order kinetic model[20] is represented by the following equation:

$$\frac{dq_t}{dt} = k_1(q_e - q_t) \tag{3}$$

where q_e is the amount of pollutant adsorbed at equilibrium in mg g^{-1}, q_t is the amount of pollutant adsorbed at time t, in mg g^{-1} and k_1 is the pseudo-first-order rate constant in min^{-1}.

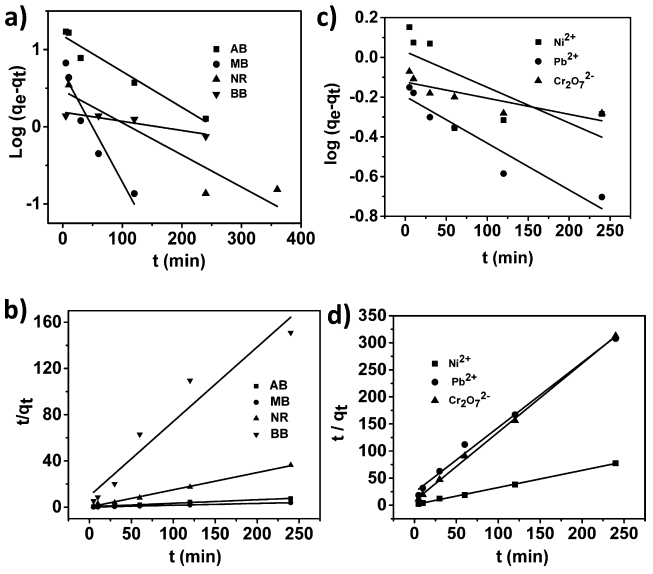

Figure 5. Pseudo-first-order (a, c) and pseudo-second-order kinetic plots (b, d) of dyes (a, b) and metal ions (c, d) adsorbed on avocado peel surface.

Upon integration of the above equation for initial and final conditions of $t = 0$ to t, $q_t = 0$ to q_t and with some rearrangement of terms, the following equation is used for data analysis:

$$\log(q_e - q_t) = \log q_e - \left(\frac{k_1}{2.303}\right)t \tag{4}$$

A linear plot of log $(q_e - q_t)$ versus t can be drawn and values of k_1 and q_e can be obtained from the slope and the intercept of the straight line graph, respectively. Figure 5 shows the graphs obtained for different dyes (Figure 5a) and metal ions (Figure 5c) adsorbed on avocado peel and Table 3 gives the values of k_1 and q_e tabulated from the plots.

Pseudo-Second-Order Kinetic Model. A pseudo-second-order reaction is used to explain the adsorption kinetics of a few systems. The pseudo-second-order kinetic model[21] is represented by the following equation:

$$\frac{t}{q_t} = \frac{1}{k_2 q_e^{\,2}} + \left(\frac{1}{q_e}\right)t \tag{5}$$

where q_e is the amount of pollutant adsorbed at equilibrium in mg g^{-1}, q_t is the amount of pollutant adsorbed at time t, in mg g^{-1} and k_2 is the pseudo-second-order rate constant in g mg^{-1} min^{-1}. A linear plot of t/q_t versus t can be drawn and values of q_e and k_2 can be obtained from the slope and the intercept of the straight line graph, respectively. The plots for the different dyes (Figure 5b) and metal ions (Figure 5d) with avocado peel are shown in Figure 5 and the calculated values of k_2 and q_e are recorded in Table 3. The calculated q_e values fit well with the

Table 2. Maximum Experimental Adsorption Capacities of Different Pollutants Using Biopeels

	adsorption capacities (mg/g)						
biopeel	AB	MB	NR	BB	Pb^{2+}	Ni^{2+}	$Cr_2O_7^{2-}$
avocado	31.04	62.11	6.88	3.23	4.93	9.82	4.89
hamimelon	66.55	58.60	6.31	4.03	7.89	9.45	0.65
dragon fruit	71.85	62.58	13.68	3.06	4.60	7.59	0.29

DOI: 10.1021/acssuschemeng.5b00207
ACS Sustainable Chem. Eng. 2015, 3, 1117−1124

Table 3. Pseudo-First-Order and Pseudo-Second-Order Constants and Correlation Coefficients for Adsorption of Different Pollutants onto Fruit Peels

(a) avocado peel							
		pseudo-first-order kinetic model			pseudo-second-order kinetic model		
pollutant	q_e (exp)	q_e (mg g^{-1})	k_1 (min^{-1})	R^2	q_e (mg g^{-1})	k_2 (g mg^{-1} min^{-1})	R^2
alcian blue	31.0424	15.1112	0.0106	0.9567	32.1543	0.0033	0.9969
methylene blue	62.0800	5.0957	0.0329	0.9276	62.1118	0.0285	1.0000
neutral red	6.8727	2.9356	0.0097	0.8648	6.7295	0.1681	0.9984
brilliant blue	2.3402	1.5481	0.0027	0.8855	1.5516	0.0432	0.9389
Pb^{2+}	4.7256	3.6308	0.0032	0.8675	3.5663	0.0077	0.9873
Ni^{2+}	9.8227	4.7087	0.0173	0.9244	10.0908	0.0111	0.9994
Cr^{6+}	3.9650	2.5960	0.0032	0.9733	3.2144	0.0111	0.9784
(b) hamimelon peel							
		pseudo-first-order kinetic model			pseudo-second-order kinetic model		
pollutant	q_e (exp)	q_e (mg g^{-1})	k_1 (min^{-1})	R^2	q_e (mg g^{-1})	k_2 (g mg^{-1} min^{-1})	R^2
alcian blue	65.9204	13.5519	0.0041	0.9230	62.8931	0.0036	0.9996
methylene blue	60.3717	25.0320	0.0078	0.7401	61.7284	0.0013	0.9973
neutral red	6.4386	2.1473	0.0067	0.6995	6.2228	0.0277	0.9985
brilliant blue	3.8101	2.8340	0.0032	0.8273	1.9964	0.1122	0.9983
Pb^{2+}	7.7243	6.5283	0.0099	0.9922	8.6655	0.0021	0.9547
Ni^{2+}	9.4751	3.5612	0.0078	0.8123	9.2851	0.0229	0.9991
Cr^{6+}	0.4169	0.2560	0.0023	0.8105	0.1693	10.9932	0.9885
(c) dragon fruit peel							
		pseudo-first-order kinetic model			pseudo-second-order kinetic model		
pollutant	q_e (exp)	q_e (mg g^{-1})	k_1 (min^{-1})	R^2	q_e (mg g^{-1})	k_2 (g mg^{-1} min^{-1})	R^2
alcian blue	71.4432	52.0236	0.0122	0.8855	78.1250	0.0004	0.9884
methylene blue	62.6123	28.4053	0.0154	0.8672	59.1716	0.0044	0.9993
neutral red	13.6892	0.5744	0.0117	0.8701	13.6799	0.0672	0.9999
brilliant blue	3.0616	2.2325	0.0076	0.7042	2.4975	0.1704	0.9683
Pb^{2+}	4.5736	0.1167	0.0014	0.4622	4.5310	0.0726	0.9998
Ni^{2+}	7.5831	1.7861	0.0108	0.8420	7.3099	0.0949	0.9975
Cr^{6+}	0.2759	0.8373	0.0101	0.6736	0.2133	0.7026	0.9835

experimental q_e values for the pseudo-second-order kinetic model. In addition, the correlation coefficient R^2 proves that the pseudo-second-order kinetic model fits the experimental data better, with values close to 1, than the pseudo-first-order kinetic model with R^2 values ranging from 0.46 to 0.99.

Isotherm Studies. The conventional adsorption isotherms are used to show the relationship between the mass of adsorbate adsorbed per unit mass of the adsorbent and the equilibrium concentration of the adsorbate. Such isotherms are meant to give some insights into adsorption process and deduce certain constants and parameters to qualify adsorption mechanism. Langumir and Freundlich isotherms describing the adsorption of different dyes and metal ions on avocado peel are given in Figure 6. All other plots for dragon fruit peels and hamimelon peels are given in the Supporting Information (Figures S6–S9).

Langmuir Isotherm. The Langmuir isotherm model is commonly used for sorption processes. It assumes that the adsorption occurs at specific homogeneous sites at the adsorbent surface and saturation is reached when the adsorbate fills up the sites and adsorption can no longer happen at those sites.[22−24] The Langmuir isotherm is expressed by the following equation:

$$q_e = \frac{K_L q_m C_e}{1 + K_L C_e} \quad (6)$$

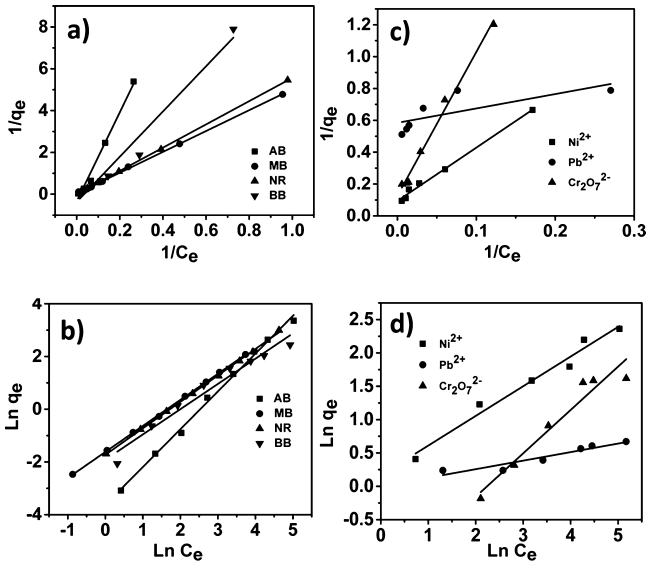

Figure 6. Langmuir (a, c) and Freundlich isotherms (b, d) of dyes (a, b) and metal ions (c, d) adsorbed on Avocado peel surface.

where q_e is the amount of adsorbate adsorbed at equilibrium in mg g^{-1}, q_m is the maximum monolayer adsorption capacity of the adsorbent in mg g^{-1}, C_e is the concentration of the adsorbate under equilibrium conditions in mg L^{-1} and K_L is the Langmuir constant in L mg^{-1}. The Langmuir isotherm can also

DOI: 10.1021/acssuschemeng.5b00207
ACS Sustainable Chem. Eng. 2015, 3, 1117−1124

Table 4. Langmuir and Freundlich Isotherm Model Constants and Correlation Coefficients for the Adsorption of the Different Pollutants on Fruit Peels

(a) avocado peel						
	Langmuir constants			Freundlich constants		
pollutant	K_L (L mg^{-1})	R_L	R^2	K_F (mg g^{-1}) (L mg^{-1})^n	$1/n$	R^2
alcian blue	0.0161	0.9688	0.9886	0.0266	1.4341	0.9963
methylene blue	0.0059	0.9884	0.9994	0.1978	0.9984	0.9997
neutral red	5.39×10^{-5}	0.9999	0.9999	0.1778	1.0034	0.9994
brilliant blue	0.0281	0.9469	0.9712	0.1474	0.9585	0.9647
Pb^{2+}	0.0257	0.9511	0.9909	0.3924	0.8772	0.9909
Ni^{2+}	0.0045	0.9912	0.9982	0.3104	1.0065	0.9993
Cr^{6+}	0.0338	0.9366	0.9928	0.3717	0.6101	0.9814
(b) hamimelon peel						
	Langmuir constants			Freundlich constants		
pollutant	K_L (L mg^{-1})	R_L	R^2	K_F (mg g^{-1}) (L mg^{-1})^n	$1/n$	R^2
alcian blue	0.0088	0.9827	0.9881	0.0393	1.3400	0.9888
methylene blue	0.0164	0.9682	0.9971	0.2045	0.9277	0.9971
neutral red	0.0039	0.9924	0.9997	0.1735	0.9882	0.9992
brilliant blue	0.0077	0.9847	0.9874	0.2308	0.8226	0.9763
Pb^{2+}	0.0063	0.9875	0.9990	0.4105	0.8824	0.9868
Ni^{2+}	0.0013	0.9975	0.9994	0.3242	0.9700	0.9935
Cr^{6+}	0.0031	0.9938	0.9994	0.1258	0.9772	0.9944
(c) dragon fruit peel						
	Langmuir constants			Freundlich constants		
pollutant	K_L (L mg^{-1})	R_L	R^2	K_F (mg g^{-1}) (L mg^{-1})^n	$1/n$	R^2
alcian blue	0.0019	0.9963	0.9971	0.1371	1.0080	0.9837
methylene blue	0.0002	0.9996	0.9999	0.1980	0.9784	0.9989
neutral red	0.0030	0.9941	0.9980	0.1654	1.0071	0.9995
brilliant blue	0.0058	0.9885	0.9981	0.2648	0.8674	0.9908
Pb^{2+}	0.0035	0.9930	0.9999	0.4408	0.8507	0.9788
Ni^{2+}	0.0038	0.9924	0.9995	0.3475	0.9568	0.9984
Cr^{6+}	0.0160	0.9690	0.9758	0.0297	1.0075	0.9811

be expressed in the following equation to determine the constants K_L and q_m:

$$\frac{1}{q_e} = \frac{1}{q_m} + \frac{1}{K_L q_m C_e} \tag{7}$$

The values of the constants can be found from the intercept and slope of the linear plots of the experimental data of $(1/q_e)$ versus $(1/C_e)$ for the different dyes (Figure 6a) and metal ions (Figure 6c), as shown in Figure 6. R^2 values are also tabulated for the observed linear relationship to be statistically significant. If the value of R^2 is close to 1, it implies that this isotherm is applicable for the extraction studies. The fundamental feature of the Langmuir isotherm can be expressed in terms of a dimensionless equilibrium parameter, such as R_L, the separation factor which is calculated using the following equation:[25]

$$R_L = \frac{1}{1 + K_L C_0} \tag{8}$$

where C_0 is the initial concentration of the adsorbate in solution in mg L^{-1}. The value of R_L indicates the adsorption process as (i) unfavorable if $R_L > 1$, (ii) linear if $R_L = 1$, (iii) favorable if $0 < R_L < 1$ and (iv) irreversible if $R_L = 0$. Table 4 shows the Langmuir isotherm constants and their correlation coefficients. The adsorption of different pollutants onto the surface of three peels was favorable as the R_L values calculated were in between 0 and 1(Table 4).

Freundlich Isotherm. The Freundlich isotherm is a model based on the adsorption of adsorbate onto heterogeneous surfaces. It is based on the assumption that the stronger binding sites are occupied first and the affinity for binding decreases with an increasing number of sites being occupied.[26,27]

The Freundlich isotherm is expressed by the following equation:

$$q_e = K_F C_e^{1/n} \tag{9}$$

where K_F and n are Freundlich constants. K_F is the adsorption capacity of the adsorbent in mg g^{-1} (L mg^{-1})^n and it represents the amount of adsorbate adsorbed onto the adsorbent for a unit equilibrium concentration. The value of $1/n$ indicates that adsorption is favorable ($n < 1$, monolayer adsorption) and a value more than 1 implies cooperative adsorption. The values of the constants can be determined from the intercept and slope of the linear plots of the experimental data of $(\ln q_e)$ versus $(\ln C_e)$ for the different dyes (Figure 6b) and metal ions (Figure6d), following the equation below:

$$\ln q_e = \ln K_F + \frac{1}{n} \ln C_e \tag{10}$$

Comparing the data in Table 4, the Langmuir isotherm model showed the best fit with the highest R^2 value of 0.99 for most of the pollutants as compared to the Freundlich isotherm model. In addition, the values of $1/n$ are less than 1 for most of the pollutants for all peels, implying that a normal Langmuir

DOI: 10.1021/acssuschemeng.5b00207
ACS Sustainable Chem. Eng. 2015, 3, 1117−1124

isotherm is applicable. The data also indicate a monolayer adsorption occurred at binding sites on the surface of the peels. The adsorption of methylene blue and neutral red onto avocado peel follows the models of both isotherms as their R^2 values were comparable.

Regeneration of Adsorbent. Adsorbents can be regenerated using desorption process. Our data indicated that biosorbents can adsorb cationic pollutants more efficiently than other type of pollutants. We investigated desorption and reusability for hamimelon peels at different pH values (4, 7 and 10) at a constant temperature of 25 °C. Only 2% desorption was observed at a pH 10, but 96% of the cationic pollutants were desorbed at pH 4 within 10 min. The peels were stable over a pH range of 4−10 and no significant weight loss, changes in morphology or changes in chemical composition of the peels were observed. However, peels started to show degradation as the pH was increased to 12 due to saponification and regeneration of the peels was done in acidic pH to maintain the extraction efficiency. Under acidic conditions, H^+ ions replace cationic pollutants from peel surface. The adsorption−desorption cycle of pollutants were repeated five times in order to show the reusability of the adsorbent using the same experimental conditions. These results showed that recycling of these peels is efficient and can be used in consecutive pollutant adsorption studies without detectable losses in their adsorption capacities. In addition, such bioadsorbents are readily available at a low cost, and helps to extract and concentrate pollutants on small amounts of adsorbents. Disposal of small amounts of pollutant adsorbed biodegradable materials can be achieved through many conventional routes.

CONCLUSIONS

Three biopeels, avocado, hamimelon and dragon fruit peels, were investigated as potential bioadsorbents for the extraction of dissolved pollutants in water. All three natural materials were effective toward removing dyes and toxic metal ions from water, reaching removal rates of 95−100%. Dragon fruit peels showed the highest extraction efficiency, close to 100%, toward alcian blue (71.85 mg/g) and methylene blue (62.58 mg/g) at neutral pH values. Hamimelon peels showed an extraction efficiency of Pb^{2+} (7.89 mg/g) and Ni^{2+} (9.45 mg/g) cations. The adsorption capacity of the pollutants increased with increasing extraction time and a plateau was reached at equilibrium, implying that the adsorption process was rapid in the beginning, gradually decreased as time progressed and finally attained saturation when equilibrium was reached. The Langmuir isotherm model fitted best the adsorption process, dominated by electrostatic interaction between adsorbent and adsorbates. The data indicate a monolayer adsorption occurrence at binding sites on the surface of the peels, yet the adsorption model of methylene blue and neutral red onto avocado peel is still a matter of conjecture. All three peels could be used as nontoxic, renewable, low cost, efficient and effective adsorbents for water purification.

ASSOCIATED CONTENT

Supporting Information

FT-IR spectra of avocado peel and hamimelon peel before and after adsorption of pollutants, and isotherms and kinetic plots of different pollutants adsorbed on hamimelon and dragon fruit peels. This material is available free of charge via the Internet at http://pubs.acs.org/.

AUTHOR INFORMATION

Corresponding Author

*S. Valiyaveettil. E-mail: chmsv@nus.edu.sg.

Notes

The authors declare no competing financial interest.

ACKNOWLEDGMENTS

The authors thank the National University of Singapore (FRC Tier 1) and Environment and Water Industry Programme Office (EWI) under the National Research Foundation of Singapore (PUBPP 21100/36/2, NUS WBS no. R-706-002-013-290, R-143-000-458-750 and R-143-000-458-731) for the financial support of the work. The authors also thank Faculty of Science, Department of Chemistry, NUS Environmental Research Institute (NERI) for funding and technical support. R.M. acknowledges NUS for a Ph.D. scholarship.

REFERENCES

(1) *The Millennium Development Goals Report*; United Nations: New York, 2008.

(2) Mohanty, K.; Das, D.; Biswas, M. N. Adsorption of phenol from aqueous solutions using activated carbons prepared from *Tectona grandis* sawdust by $ZnCl_2$ activation. *Chem. Eng. J.* **2005**, *115*, 121−131.

(3) Hossain, M. A.; Kumita, M.; Michigami, Y.; Mori, S. Optimization of parameters for Cr(VI) adsorption on used black tea leaves. *Adsorption* **2005**, *11*, 561−568.

(4) Veglio, F.; Beolchini, F. Removal of metals by biosorption: A review. *Hydrometallurgy* **1997**, *44*, 301−316.

(5) Crini, G. Non-conventional low-cost adsorbents for dye removal: A review. *Bioresour. Technol.* **2006**, *97*, 1061−1085.

(6) Vinod, V. T. P.; Sashidhar, R. B.; Sreedhar, B. Biosorption of nickel and total chromium from aqueous solution by gum kondagogu (*Cochlospermum gossypium*): A carbohydrate biopolymer. *J. Hazard. Mater.* **2010**, *178*, 851−860.

(7) O'Neill, C.; Hawkes, F. R.; Hawkes, D. L.; Lourenço, N. D.; Pinheiro, H. M.; Delée, W. Colour in textile effluents − Sources, measurement, discharge consents and simulation: A review. *J. Chem. Technol. Biotechnol.* **1999**, *74*, 1009−1018.

(8) Vandevivere, P. C.; Bianchi, R.; Verstraete, W. Review: Treatment and reuse of wastewater from the textile wet-processing industry: Review of emerging technologies. *J. Chem. Technol. Biotechnol.* **1998**, *72*, 289−302.

(9) Castro, E.; Avellaneda, A.; Marco, P. Combination of advanced oxidation processes and biological treatment for the removal of benzidine-derived dyes. *Environ. Prog. Sust. Energ.* **2014**, *33*, 873−885.

(10) Kumar, U.; Bandyopadhyay, M. Sorption of cadmium from aqueous solution using pretreated rice husk. *Bioresour. Technol.* **2006**, *97*, 104−109.

(11) Nawar, S. S.; Doma, H. S. Removal of dyes from effluents using low-cost agricultural by-products. *Sci. Total Environ.* **1989**, *79*, 271−279.

(12) Ali, A.; Saeed, K. Decontamination of Cr(VI) and Mn(II) from aqueous media by untreated and chemically treated banana peel: A comparative study. *Desal. Water Treat.* **2015**, *53*, 3586−3591.

(13) Xuli, G. F.; Shen, Z. X.; Guo, R. X. The kinetic studies for the adsorption of furdan from aqueous solution by orange peel. *Adv. Mater. Res.* **2014**, *842*, 187−191.

(14) Malkoc, E.; Nuhoglu, Y. Investigations of nickel(II) removal from aqueous solutions using tea factory waste. *J. Hazard. Mater.* **2005**, *127*, 120−128.

(15) Malkoc, E.; Nuhoglu, Y. Fixed bed studies for the sorption of chromium(VI) onto tea factory waste. *Chem. Eng. Sci.* **2006**, *61*, 4363−4372.

(16) Garg, U. K.; Kaur, M. P.; Garg, V. K.; Sud, D. Removal of hexavalent chromium from aqueous solution by agricultural waste biomass. *J. Hazard. Mater.* **2007**, *140*, 60−68.

DOI: 10.1021/acssuschemeng.5b00207
ACS Sustainable Chem. Eng. 2015, 3, 1117−1124

(17) Al-Asheh, S.; Banat, F.; Al-Omari, R.; Duvnjak, Z. Predictions of binary sorption isotherms for the sorption of heavy metals by pine bark using single isotherm data. *Chemosphere* **2000**, *41*, 659−665.
(18) Agarwal, G. S.; Bhuptawat, H. K.; Chaudhari, S. Biosorption of aqueous chromium(VI) by *Tamarindus indica* seeds. *Bioresour. Technol.* **2006**, *97*, 949−956.
(19) Devi Prasad, A. G.; Abdullah, M. Biosorption of Fe(II) from aqueous solution using Tamarind Bark and potato peel waste: Equilibrium and kinetic Studies. *J. Appl. Sci. Environ. Sanit.* **2009**, *4*, 273−282.
(20) Koel Banerjee, S. T.; Ramesh, R.; Gandhimathi, P. V.; Bharathi, K. S. A novel agricultural waste adsorbent, watermelon shell for the removal of copper from aqueous solutions. *Iran. J. Energy* **2012**, *3*, 143−156.
(21) Venkateswarlu, P.; Ratnam, M. V.; Rao, D. S.; Rao, M. V. Removal of chromium from an aqueous solution using *Azadirachta indica* (neem) leaf powder as an adsorbent. *Int. J. Phys. Sci.* **2007**, *2*, 188−195.
(22) Altun, T.; Pehlivan, E. Removal of copper(II) ions from aqueous solutions by walnut-, hazelnut- and almond-shells. *CLEAN − Soil, Air, Water* **2007**, *35*, 601−606.
(23) Saeed, A.; Iqbal, M.; Akhtar, M. W. Removal and recovery of lead(II) from single and multimetal (Cd, Cu, Ni, Zn) solutions by crop milling waste (black gram husk). *J. Hazard. Mater.* **2005**, *117*, 65−73.
(24) Feng, Y.; Yang, F.; Wang, Y.; Ma, L.; Wu, Y.; Kerr, P. G.; Yang, L. Basic dye adsorption onto an agro-based waste material − Sesame hull (*Sesamum indicum* L.). *Bioresour. Technol.* **2011**, *102*, 10280−10285.
(25) Mallampati, R.; Valiyaveettil, S. Application of tomato peel as an efficient adsorbent for water purification—Alternative biotechnology? *RSC Adv.* **2012**, *2*, 9914−9920.
(26) Negi, R.; Satpathy, G.; Tyagi, Y. K.; Gupta, R. K. Biosorption of heavy metals by utilising onion and garlic wastes. *Int. J. Environ. Pollut.* **2012**, *49*, 179−196.
(27) Tang, P. Y.; Wong, C. J.; Woo, K. K. Optimization of pectin extraction from peel of dragon fruit (*Hylocereus polyrhizus*). *Asian J. Biol. Sci.* **2011**, *4*, 189−195.
(28) Haris, M. R. H. M.; Sathasivam, K. The removal of methyl red from aqueous solutions using banana pseudostem fibers. *Am. J. Appl. Sci.* **2009**, *6*, 1690−1700.
(29) Salleh, M. A. M.; Mahmoud, D. L.; Awang Abu, N. A. B.; Abdul Karim, W. A. W.; Idris, A. B. Methylene blue adsorption from aqueous solution by langsat (*Lansium domesticum*) peel. *J. Purity, Util. React. Environ.* **2012**, *1*, 472−495.
(30) Chand, R.; Narimura, K.; Kawakita, H.; Ohto, K.; Watari, T.; Inoue, K. Grape waste as a biosorbent for removing Cr(VI) from aqueous solution. *J. Hazard. Mater.* **2009**, *163*, 245−250.
(31) Homagai, P. L.; Ghimire, K. N.; Inoue, K. Adsorption behavior of heavy metals onto chemically modified sugarcane bagasse. *Bioresour. Technol.* **2010**, *101*, 2067−2069.
(32) Rouffa, A.; Elzinga, E. J.; Reeder, R. J; Fisher, N. S. The influence of pH on the kinetics, reversibility and mechanisms of Pb(II) sorption at the calcite-water interface. *Geochim. Cosmochim. Acta* **2015**, *69*, 5173−5186.
(33) Reddy, K.; Al-hamdan, Z. Surface speciation modeling of heavy metals in kaolin: Implications for electrokinetic soil remediation processes. *Adsorption* **2015**, *11*, 529−546.
(34) Nakajima, A.; Baba, Y. Mechanism of hexavalent chromium adsorption by persimmon tannin gel. *Water Res.* **2004**, *38*, 2859−2864.

DOI: 10.1021/acssuschemeng.5b00207
ACS Sustainable Chem. Eng. 2015, 3, 1117−1124